Electronic Supplementary Information

Nitrogen/fluorine-codoped rutile titania as a stable oxygen-evolution photocatalyst for solar-driven Z-scheme water splitting

Akinobu Miyoshi,[a] *Junie Jhon M. Vequizo,*[b] *Shunta Nishioka,*[a,c] *Yuma Kato,*[d] *Muneaki Yamamoto,*[e] *Shunsuke Yamashita,*[f] *Toshiyuki Yokoi,*[g] *Akihide Iwase,*[h,i] *Shunsuke Nozawa,*[j] *Akira Yamakata,*[b] *Tomoko Yoshida,*[d] *Koji Kimoto,*[f] *Akihiko Kudo,*[h,i] *and Kazuhiko Maeda**[a]

[a] Department of Chemistry, School of Science, Tokyo Institute of Technology, 2-12-1-NE-2 Ookayama, Meguro-ku, Tokyo 152-8550, Japan.

[b] Graduate School of Engineering, Toyota Technological Institute, 2-12-1 Hisakata, Tempaku, Nagoya 468-8511, Japan.

[c] Japan Society for the Promotion of Science, Kojimachi Business Center Building, 5-3-1, Kojimachi, Chiyoda-ku, Tokyo 102-0083, Japan.

[d] Advanced Research Institute for Natural Science and Technology, Osaka City University, 3-3-138 Sugimoto Sumiyoshi-ku, Osaka, 558-8585, Japan.

[e] Institute of Materials and Systems for Sustainability, Nagoya University, Furo-cho, Chikusa-ku, Nagoya 464-8603, Japan.

[f] Electron Microscopy Group, Research Center for Advanced Measurement and Characterization, National Institute for Materials Science, 1-1 Namiki, Tsukuba 305-0044, Japan.

[g] Nanospace Catalysis Unit, Institute of Innovative Research, Tokyo Institute of Technology, 4259 Nagatsuta, Midori-ku, Yokohama 226-8503, Japan.

[h] Department of Applied Chemistry, Faculty of Science, Tokyo University of Science, 1-3 Kagurazaka, Shinjuku-ku, Tokyo 162-8601, Japan.

[i] Photocatalysis International Research Centre, Research Institute for Science and Technology, Tokyo University of Science, 2641 Noda-shi, Yamazaki, Chiba 278-8510, Japan.

[j] Institute of Materials Structure Science, High Energy Accelerator Research Organization, 1-1 Oho, Tsukuba, Ibaraki 305-0801, Japan.

*To whom corresponding author should be addressed.

TEL: +81-3-5734-2239, FAX: +81-3-5734-2284

Email: maedak@chem.titech.ac.jp

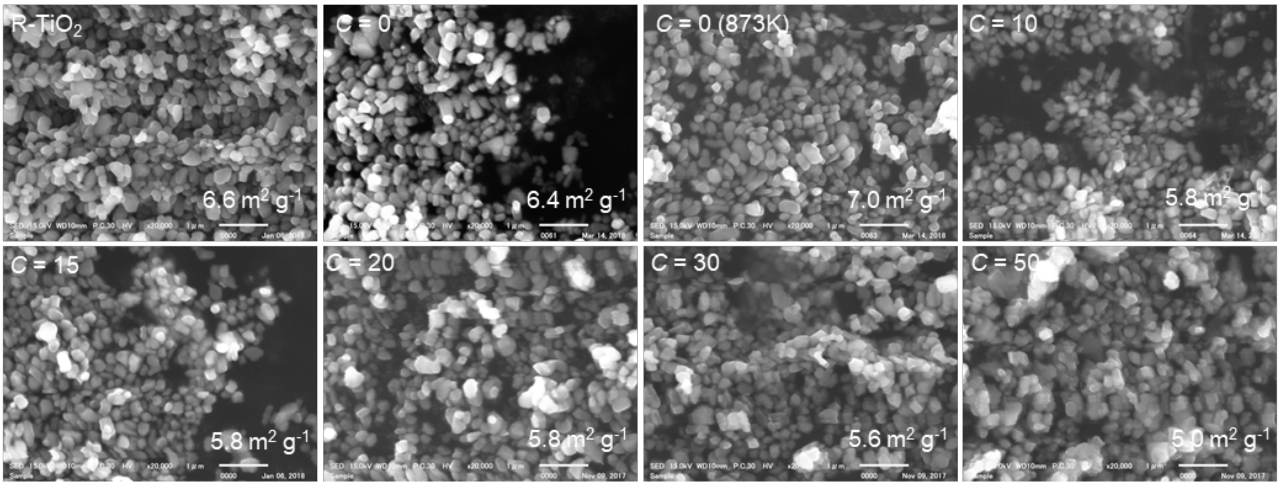

Fig. S1. SEM images of R-TiO_2:N,F with different *C* values.

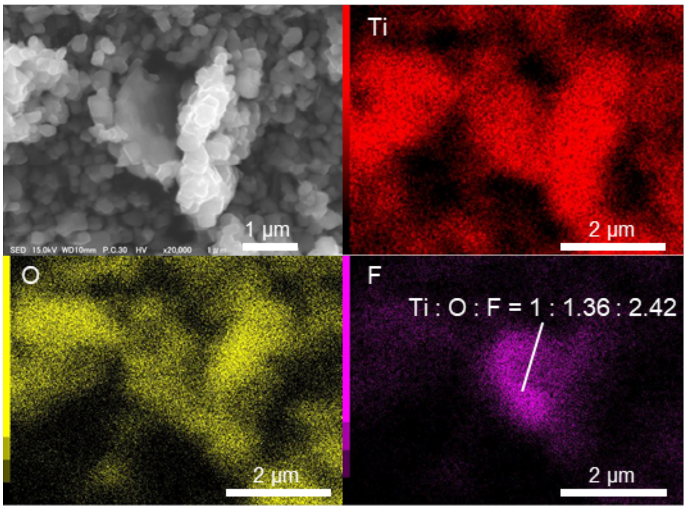

Fig. S2. SEM image and EDX elemental mapping of fluorine rich particle in R-TiO_2:N,F (*C* = 50).

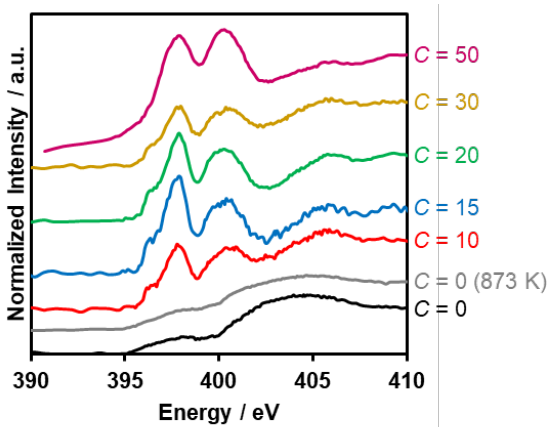

Fig. S3. N-K edge XANES of R-TiO_2:N,F with various *C* values.

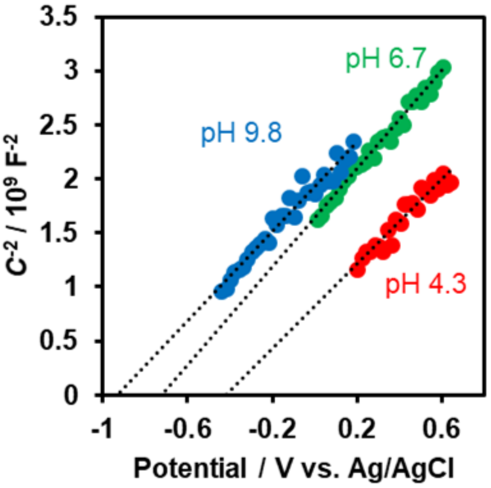

Fig. S4. Mott-Schottky plots of R-TiO$_2$:N,F (C = 15) recorded at different pH values. Impedance frequency was 100 Hz.

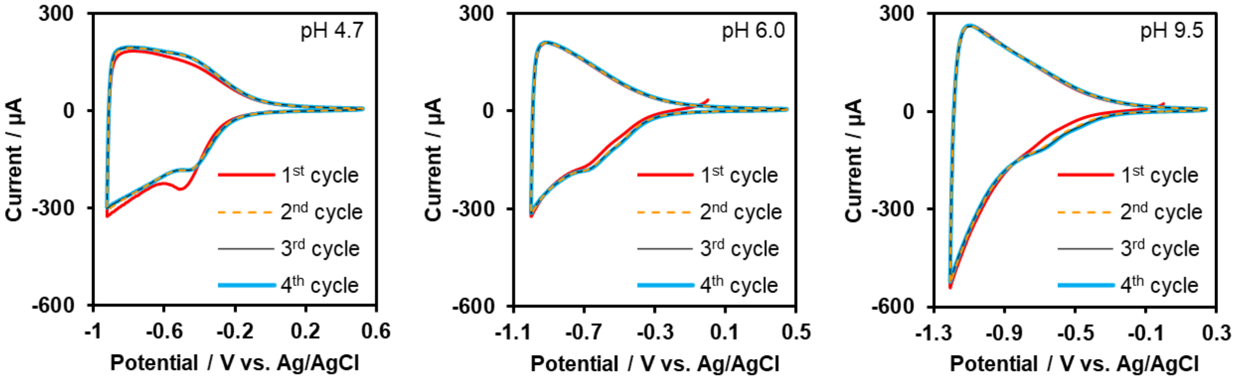

Fig. S5. Cyclic voltammograms of R-TiO$_2$:N,F (C = 15)/FTO electrode measured in Na_2SO_4 aqueous electrolyte solution at different pH values in the dark. The shape of CV profiles at each pH became constant with increasing the scan times (after the second scan), indicating that the electrode is electrochemically stable at the pH range examined.

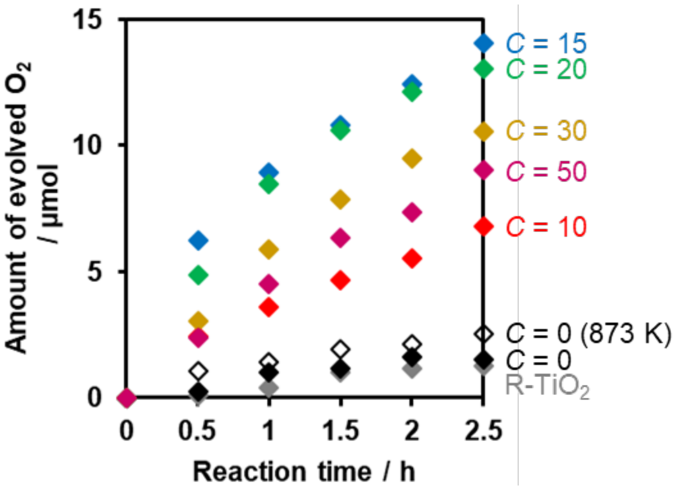

Fig. S6. Time courses of O_2 evolution on R-TiO$_2$:N,F with different C values under visible light irradiation in $AgNO_3$ aqueous solution. Reaction conditions: catalyst, 50 mg; La_2O_3 200 mg; 10 mM $AgNO_3$ aqueous solution, 140 mL; light source, 300 W Xe lamp fitted with CM-1 mirror and L42 cutoff filter ($\lambda > 420$ nm).

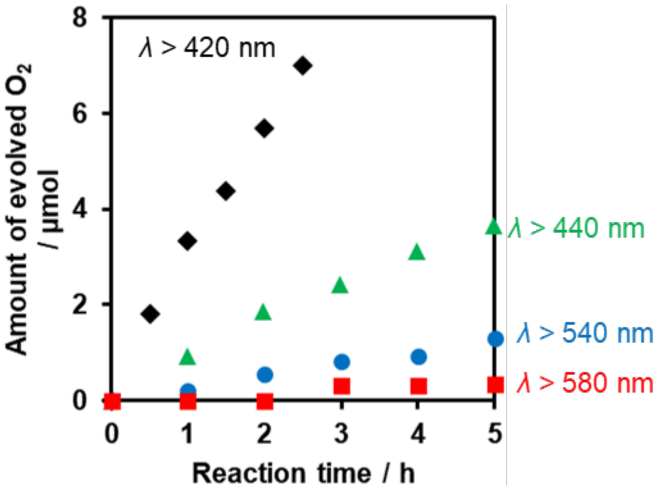

Fig. S7. Photocatalytic activity of R-TiO_2:N,F for O_2 evolution under visible light irradiation with various wavelength in $AgNO_3$ aqueous solution. Reaction conditions: catalyst, 50 mg; La_2O_3 200 mg; 10 mM $AgNO_3$ aqueous solution, 140 mL; light source, 300 W Xe lamp fitted with CM-1 mirror and various cutoff filters (L42, Y44, O54, O58). Output current of the Xe lamp was 10 A.

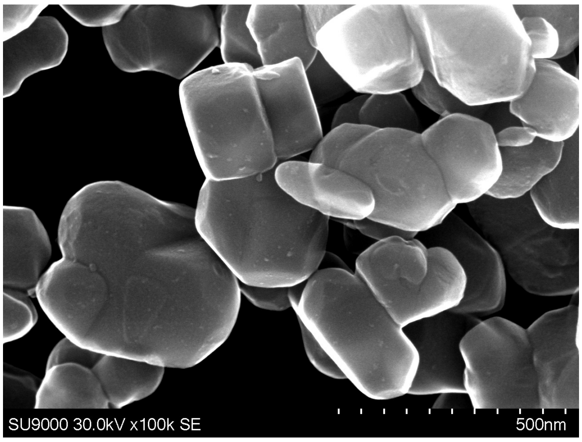

Fig. S8. SEM image of RuO_2-loaded R-TiO_2:N,F ($C = 15$).

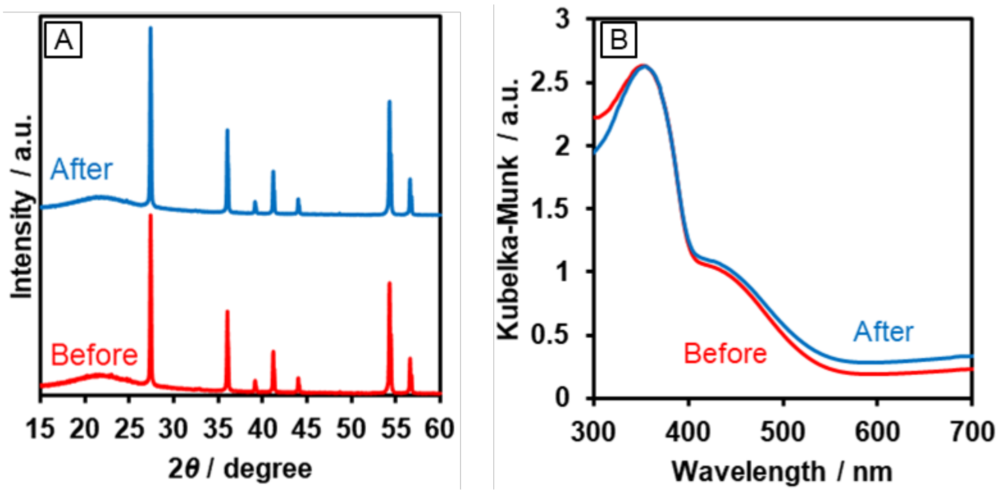

Fig. S9. (A) XRD and (B) DRS of RuO_2/R-TiO_2:N,F before and after the oxygen evolution reaction from $NaIO_3$ aqueous solution.

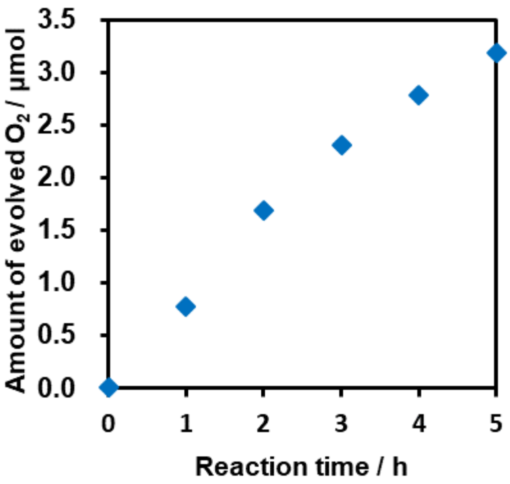

Fig. S10. Time course of O_2 evolution during photocatalytic reaction of RuO_2/R-TiO_2:N,F ($C = 15$) under visible light irradiation in $FeCl_3$ aqueous solution. Reaction conditions: catalyst, 50 mg; 10 mM $FeCl_3$ aqueous solution (pH 2.3), 140 mL; light source, 300 W xenon lamp fitted with CM-1 mirror and L42 cutoff filter ($\lambda > 420$ nm).

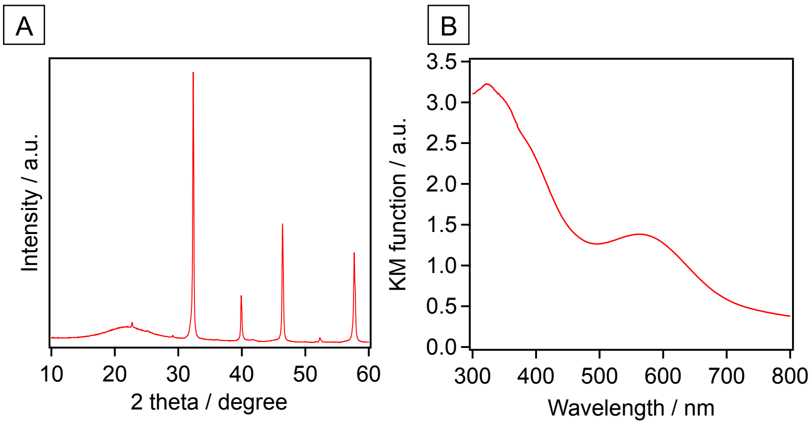

Fig. S11. (A) XRD pattern and (B) UV-visible diffuse reflectance spectrum of the as-prepared $SrTiO_3$:Rh.

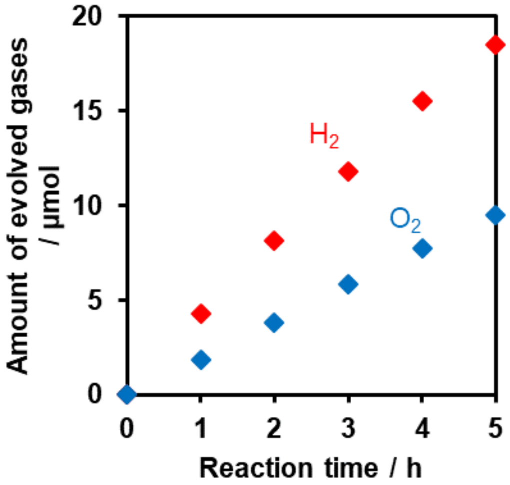

Fig. S12. Time course of H_2 and O_2 evolution from mixtures of RuO_2/R-TiO_2:N,F ($C = 15$) (50 mg) and Ru/$SrTiO_3$:Rh (25 mg) dispersed in an aqueous solution (120 mL) containing tris(2,2'-bipyridyl)cobalt(II) sulfate (0.5 mM) under AM1.5G irradiation (0.1 W cm^{-2}).

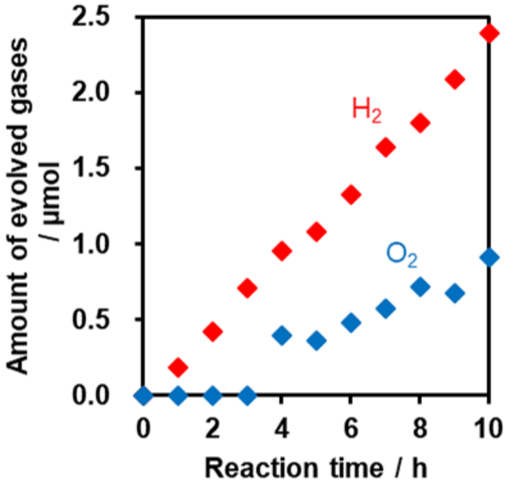

Fig. S13. Time course of H_2 and O_2 evolution from mixtures of RuO_2/R-TiO_2:N,F ($C = 15$) (50 mg) and Ru/$SrTiO_3$:Rh (25 mg) dispersed in pure water (120 mL) under visible-light irradiation ($\lambda > 420$ nm).

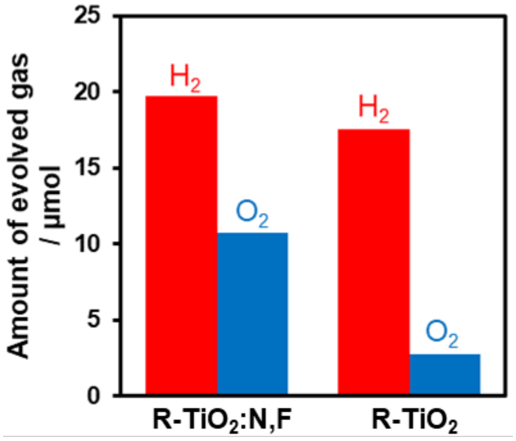

Fig. S14. Amounts of H_2 and O_2 evolved from mixtures of RuO_2/R-TiO_2 (50 mg) and Ru/$SrTiO_3$:Rh (25 mg) dispersed in an aqueous solution (120 mL) containing tris(2,2'-bipyridyl)cobalt(II) sulfate (0.5 mM) under visible-light irradiation ($\lambda > 440$ nm) after 10 h. Here a Y44 cutoff filter was employed. Data for the RuO_2/R-TiO_2:N,F-based system is also shown for comparison.

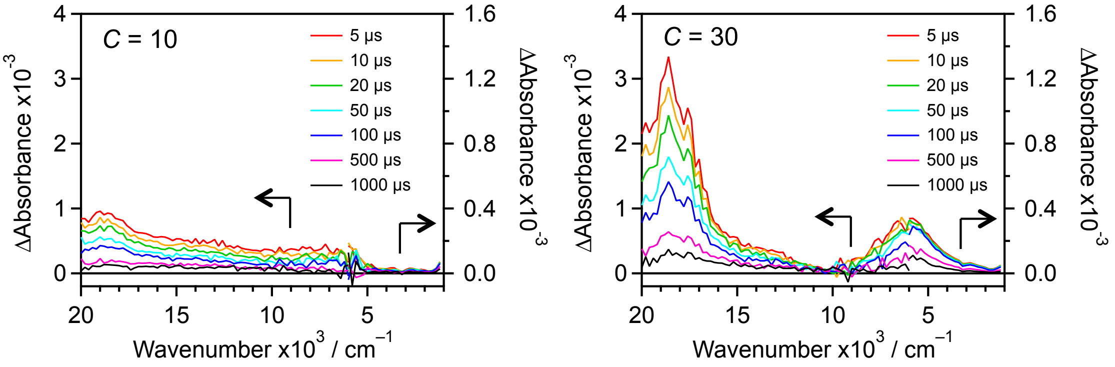

Fig. S15. Transient absorption spectra for R-TiO_2:N,F with different C values excited with 480 nm laser pulses under N_2 atmosphere. Transmittance and reflectance were measured below and above 6000 cm^{-1}, respectively.

Table S1. Surface atomic ratios of R-TiO_2:N,F ($C = 15$) determined by XPS analysis.

N/Ti	O/Ti	F/Ti	Ni/Ti
0.11	2.72	0.43	0.02